European Radiology (2019) 29:279–286
https://doi.org/10.1007/s00330-018-5558-0

CHEST

CT diagnosis of pleural and stromal invasion in malignant subpleural pure ground-glass nodules: an exploratory study

Qing Zhao[1] · Jian-wei Wang[1] · Lin Yang[2] · Li-yan Xue[2] · Wen-wen Lu[1]

Received: 4 February 2018 / Revised: 23 April 2018 / Accepted: 23 May 2018 / Published online: 25 June 2018

Abstract

Objectives To assess the risk of visceral pleural invasion (VPI) and improve the diagnosis of invasive adenocarcinoma (IA) in pure ground-glass nodules (pGGNs) in contact with pleura, through a comprehensive analysis of the thin-section CT features of subpleural malignant pGGNs.

Methods CT findings and clinical information of 115 consecutive patients in our hospital between January 2012 and December 2015 who met the following criteria were retrospectively studied: (a) thin-section CT within 1 month before surgery proved pGGN in contact with pleura, and (b) the pGGN was confirmed as malignancy by surgery. Univariate analysis and a multivariate logistic regression analysis were conducted to identify the independent risk factors of IA and VPI.

Results No pleural invasion was observed microscopically in any of the pGGNs. Univariate analysis indicated that tumour shape ($p = 0.004$), relative density ($p = 0.038$) and the existence of pleural retraction ($p < 0.001$) were significantly different between the invasive group and pre- or minimally invasive group. Multivariate logistic regression analysis revealed that pleural retraction (OR, 5.663; $p < 0.001$), lobulated tumour shape (OR, 4.812; $p = 0.016$) and tumour relative density greater than 1.60 (OR, 4.449; $p = 0.001$) were independent risk factors of IA.

Conclusions Pulmonary adenocarcinoma manifesting as pGGN generally does not invade the pleura. A comprehensive consideration of tumour shape, relative density and tumour–pleural relationship can independently predict IA.

Key Points

- *This study showed that pGGN-like adenocarcinoma generally does not invade the pleura.*
- *This study suggested that persistent pGGN with pleural retraction, lobulated shape and high relative density (> 1.60) may very likely be invasive adenocarcinoma.*
- *Using "relative density" can reduce confounding of contrast agent and respiratory status in analysis of CT images.*

Keywords Lung neoplasms · Solitary pulmonary nodule · Visceral pleura · Relative density

Abbreviations

AAH	Adenomatous hyperplasia
AIS	Adenocarcinoma in situ
GGN	Ground-glass nodule
HE	Haematoxylin–eosin
HRCT	High-resolution computed tomography
IA	Invasive adenocarcinoma
mGGN	Mixed ground-glass nodule
MIA	Minimally invasive adenocarcinoma
NSCLC	Non-small cell lung carcinoma
PACS	Picture Archiving and Communication System
pGGN	Pure ground-glass nodule
pre-IA	Pre-invasive adenocarcinoma
VPI	Visceral pleural invasion

✉ Jian-wei Wang
dr_jianweiwang@163.com

[1] Department of Diagnostic Radiology, National Cancer Center/Cancer Hospital, Chinese Academy of Medical Sciences and Peking Union Medical College, 17 Pan Jia Yuan Nan-li, Beijing 100021, China

[2] Department of Diagnostic Pathology, National Cancer Center/Cancer Hospital, Chinese Academy of Medical Sciences and Peking Union Medical College, 17 Pan Jia Yuan Nan-li, Beijing 100021, China

Introduction

With the popularisation of low-dose CT screening of the lung, ground-glass nodules (GGNs) have increasingly been

detected and received more and more attention because of the potential malignancy they may represent [1, 2]. GGN is defined as a nodule of slight increase in density, without obscuring underlying bronchial structures or vascular margins on high-resolution CT (HRCT) [3]. On the basis of the presence of solid components, GGNs can be classified into pure GGN (pGGN) and mixed GGN (mGGN). Persistent GGNs always confer a high risk of adenocarcinoma [4]. According to the 2015 WHO pathological classification of lung tumours [5], adenocarcinomas are divided into three broad groups: pre-invasive lesions (pre-IA) which include atypical adenomatous hyperplasia (AAH) and adenocarcinoma in situ (AIS); minimally invasive adenocarcinoma (MIA); and invasive adenocarcinoma (IA). Both pre-IA and MIA are considered to grow very slowly and have a favourable prognosis, mostly presenting as pGGNs on HRCT. But at the same time, pGGNs can also exhibit higher invasiveness [6–13], which may call for more intensive surveillance and more active treatment, as well as more accurate preoperative diagnosis. Some researchers suggested that pGGNs with greater tumour size, high pixel attenuation, unsmooth margin or pleural indentation on HRCT were more likely to be IA [7–11]. However, these studies still could not result in a definite criterion to integrate the contribution of different risk factors to achieve a probabilistic forecast of IA in pGGNs.

In addition, more importantly, although the adverse prognostic implications of visceral pleural invasion (VPI) in solid non-small cell lung carcinoma (NSCLC) have been well recognised in the past decades [14–23], it is still unclear whether VPI would happen in pGGNs and what the CT manifestation would be. Some researchers speculated that VPI would not happen in pGGNs [24] and even would not impact the prognosis of patients with mGGN-like NSCLCs [25] owing to the minimally invasive nature of the "ground glass" component, but evidence was still not enough to draw any strong conclusions. In clinical practice, on account of the suspected VPI, it is still recommended that pGGNs in contact with pleura should trigger immediate resection, which may lead to over-treatment.

So, it is of clinical relevance to get a better understanding of the pleural and stromal invasiveness of pGGNs to facilitate the surveillance strategy and surgery in patients with persistent pGGNs. Herein, we report a retrospective study of patients with subpleural pGGNs which were identified in preoperative thin-section CT and confirmed malignant by surgery, to explore the existence and CT manifestation of VPI in pGGNs, as well as to facilitate the CT diagnosis of IA.

Materials and methods

This retrospective study was approved by our institutional review board with a waiver of informed consent. The CT findings, pathological and clinical information for patients who met all the following criteria and received resection in our hospital between January 2012 and December 2015 were retrospectively reviewed: (a) preoperative thin-section CT showed subpleural pGGN lesion attached or connected by streaks with (costal, mediastinal, diaphragmatic or interlobar) pleural surface, (b) pathologically confirmed primary lung malignancies, including the pre-invasive subtypes and (c) tumour resection performed within 1 month after the CT scan. pGGN was defined as a pulmonary nodule completely composed of hazy increased opacity, with preservation of underlying bronchial and vascular margins [26]. In total, 137 patients met the inclusion criteria. For fear of the confusable streaks and pleural morphologic changes, those with a history of interstitial or granulomatous lung diseases were excluded, which accounted for 22 patients. Finally, 115 patients were enrolled in this study.

CT scanning and image reconstruction

Chest CT was performed with two 64-row CT scanners (75 patients with GE Discovery CT750 HD; 40 patients with GE Lightspeed VCT). The range of the scans included the upper supraclavicular area and the lower adrenal area on both sides. The scanning parameters were 120 kVp and auto milliampere settings (tube current, 200 mA; noise index, 13; pitch, 0.984:1; 40 mm/rotation; 1.25-mm slice thickness; 0.8 s/rotation). In 53 patients, non-ionic contrast medium (1.5 mL/kg, 300 mgI/mL; Bayer Schering, Berlin, Germany) was administered intravenously at a rate of 3 mL/s. The other 62 cases were scanned without the administration of contrast medium. The raw data were reconstructed at section widths of 1.25 mm with an interval of 0.8 mm using standard and high-resolution reconstruction filters. All CT scans were obtained at full inspiration.

CT images were reviewed individually by two radiologists (Q.Z. and J.W.W, with 5 and 22 years of chest imaging experience, respectively) on PACS, blinded to the clinicopathological information. Differences in their findings were resolved by discussion until reaching a consensus. The following features were examined: location of the lesion; the largest diameter on multiplanar reconstruction (MPR) images, tumour volume and calculated tumour mass; tumour density and relative density [27] (CT attenuation of normal lung parenchyma/tumour attenuation); tumour shape (round/oval or lobulated), contour (smooth or coarse), the tumour–pleural relationship and the existence of thickened pleura. All CT images were posted back from PACS to the workstation (Advantage Windows 4.6, GE Healthcare), where the volume of each nodule was measured with LungVCAR software (GE Healthcare) [28]. Tumour mass was calculated according

the following formula: mass = tumour volume × (1000 + tumour density)/10^6 [29]. Tumour density was calculated by averaging three or more measured CT attenuation values in different sections of the nodule, and attenuation of normal lung field was measured in the layer of the tumour centre, within the same lobe, avoiding vessels and bronchi. A lobulated shape was defined as polygonal or non-geometric, not round or oval (Fig. 1). The relationship between pGGN and pleura was classified into three subgroups according to pleural deformation: 1, pleural attachment [30]—tumour margin attaches to the pleura but without pleural distortion (Fig. 1a); 2, pleural tag [31, 32]—one or more linear strands radiating from the mass distal from the pleura to the pleural surface, with or without pleural folding (Fig. 1b, c); and 3, pleural indentation [31, 33]—tentiform indrawing of the pleura toward the deep inside of the tumour from the broad tumour–pleura interface (> 50% of the largest diameter) (Fig. 1d, e). When there were several points of contact with the pleura, the highest group number was recorded. Pleural thickening was evaluated on 1.25-mm-section CT images with mediastinal window settings (window width, WW, 350–600 HU; window level, WL, 30–60 HU), and the other parameters were assessed on 1.25-mm-section CT images with lung window settings (WW, 1000–2000 HU; WL, − 500 to − 700 HU).

Surgery

Out of the enrolled cases, 48 were treated with segmentectomy or sublobectomy plus nodal dissection, and 67 cases underwent wedge resection without nodal dissection.

Pathological evaluation and TNM staging

Pathology re-evaluation was performed by two pathologists (L.Y. and L.Y.X., both with 15 years of experience) on the basis of the 2015 WHO pathological classification of lung tumours [5] in this study. All dissected tumours and lymph nodes were sectioned and examined conventionally by haematoxylin–eosin (HE) staining.

VPI was confirmed by Elastica–Masson and elastic staining, ranging from PL0 to PL3 [34]: PL0, no pleural invasion; PL1, invasion beyond the elastic layer of the visceral pleura without reaching the pleural surface; PL2, invasion to the visceral pleural surface without involving adjacent anatomic structures; and PL3, invasion to the parietal pleura. TNM stage was determined according to the 7th edition of the UICC (Union for International Cancer Control) TNM classification [35].

Statistical analysis

The CT characteristics and clinicopathological parameters, including age, sex, smoking status, histological subtypes, VPI, lymph node metastasis (LNM) and TNM stages, were analysed. The variables were described as the mean ± standard deviation (range) or number (proportion). The Kolmogorov–Smirnov test was used to evaluate whether the measurable variables were normally distributed. Unpaired *t* test was used for normally distributed variables, and Kruskal–Wallis variance analysis and Mann–Whitney *U* tests were used for non-normally distributed variables. A χ^2 test or Fisher exact test was used to test the differences in the CT features between the groups with

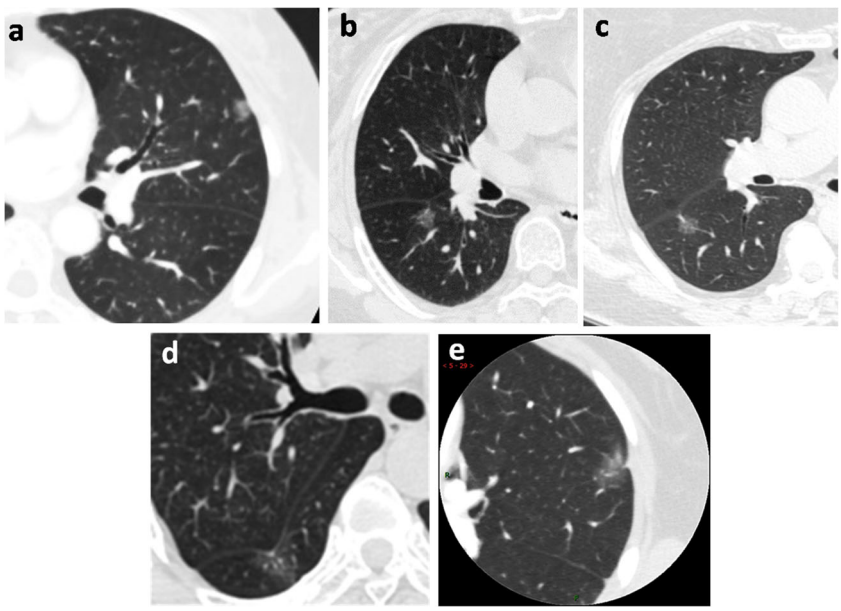

Fig. 1 pGGN shape description and nodule–pleural relationships. **a** Lobulated shape, pleural attachment without pleural distortion; **b** lobulated shape, pleural tag with pleural folding; **c** round shape, pleural tag without pleural folding; **d** lobulated shape, pleural retraction showing enfoldment of the pleura into the tumour; **e** lobulated shape, tentiform indrawing of the pleura toward the tumour

and without pleural invasion. Receiver operating characteristic curve (ROC) analysis was also performed to evaluate the cut-off and differentiate the performance of significant continuous variables. Finally, a multivariable logistic regression analysis (backward conditioning) was then conducted, involving the variables that were statistically significant in previous analysis to identify the independent factors predicting IA. All analyses were conducted using IBM SPSS Statistics (version 22.0, IBM, Armonk, NY). A value of $p < 0.05$ indicated a statistically significant difference. The interobserver variability was assessed using κ statistics. A κ value less than 0.40 indicated poor agreement; 0.40–0.59, moderate agreement; 0.60–0.74, good agreement; and 0.75 or greater, excellent agreement [36].

Results

Among the 115 cases, the ratio of women to men was approximately 3:1, with an average age of 56.4 ± 10.3 years. Only 12 patients (10.4%) had a history of smoking, with the others all being non-smokers. Adenocarcinoma was the only pathological type, with 47 IA, 36 MIA and 32 AIS. Most strikingly, none of the lesions had invaded the visceral pleura (all being PL0). The patients' demographics together with pathologic findings are listed in Table 1.

On the basis of tumour prognosis, the patients were divided into IA and pre-IA/MIA groups. Univariate analysis revealed that lobulated tumour shape ($p = 0.002$) and pleural indentation ($p < 0.001$) were differently distributed in the two groups, and a higher relative density was also found in the IA group (1.68 ± 0.21 vs. 1.56 ± 0.17, $p = 0.038$). Whereas, there was no significant difference in patient age, sex, smoking status, tumour location, largest diameter, TV, TD, contour and other tumour–pleural relationships (Table 2). The ROC analysis for relative density confirmed a cut-off value of 1.60 which yielded the highest combined sensitivity (Sen = 72.3%) and specificity (Spe = 64.7%) with respect to distinguishing IA independently. The subsequent multivariate logistic regression analysis revealed that lobulated tumour shape, pleural retraction and a relative density greater than 1.60 were independent predictors of IA; the ORs and probabilities are presented in Table 3. In addition, the determination of lobulation ($\kappa = 0.796$, $p < 0.001$) and positive pleural retraction ($\kappa = 0.803$, $p < 0.001$) were both highly consistent between different observers.

Discussion

The present study explored the existence and diagnosis of VPI in malignant pGGNs for the first time and found that this type of indolent tumour generally does not invade the pleura. Meanwhile, the study also indicated that a comprehensive consideration of the tumour shape, relative density and the tumour–pleural relationship can be a powerful supportive tool for radiologists to distinguish IA (Fig. 2a–e).

The visceral pleura is very rich in lymphatic vessels with drainage to various hilar lymph nodes [16], which, if invaded, can increase the risk of locoregional recurrence and systemic metastases [37, 38]. The 5-year survival rates were reported to worsen from 86% for patients with pl0 to 62–70% for patients with pl1 or pl2, and then to 57% for patients with pl3 for solid NSCLCs [23]. Previous studies have revealed that pleural retraction is closely associated with higher invasiveness or VPI in NSCLCs [8, 31, 32, 39–43]. However, all of these studies

Table 1 Patients and tumour characteristics

Variable		Data
No. of patients		115
Sex	Men	29
	Women	86
Ever smokers, *n* (%)		12 (10.4%)
Age, mean ± SD (range), years		56.4 ± 10.3
Tumour subtype	Invasive adenocarcinoma (IA)	47
	Minimally invasive adenocarcinoma (MIA)	36
	Adenocarcinoma in situ (AIS)	32
Visceral pleural invasion (VPI)	Positive	0
	Negative	115
Lymph node metastasis (LNM)		0

Data are numbers (%) and mean ± standard deviation

Table 2 Univariate analysis results

Factor			IA	Pre-IA/MIA	Total	*p*
Percentage of women			72.3%	76.5%	74.8%	0.618
Age, years			54.8 ± 9.4	57.5 ± 10.7	56.4 ± 10.3	0.152
Ever smokers, *n* (%)			6 (12.8%)	6 (8.8%)	12 (10.4%)	0.498
Tumour location	RUL		14	17	31	0.639
	RML		7	8	15	
	RLL		2	10	12	
	LUL		17	22	39	
	LLL		7	11	18	
Largest diameter, mm			14.6 ± 3.4	14.3 ± 4.2	14.4 ± 3.9	0.679
Volume, mm^3			856.1 ± 514.4	822.0 ± 636.0	835.9 ± 587.8	0.752
Calculated mass			0.42 ± 0.25	0.39 ± 0.32	0.40 ± 0.29	0.599
Shape	Round and oval		4	21	25	0.004
	Lobulated		43	47	90	
Contour	Smooth		32	56	88	0.253
	Coarse		15	12	27	
Average tumour density, Hounsfield units			– 506.7 ± 72.9	– 531.7 ± 76.0	– 521.5 ± 75.5	0.078
Normal lung density, Hounsfield units			– 854.6 ± 40.3	– 843.1 ± 38.1	– 847.8 ± 39.2	0.128
Relative density			1.72 ± 0.24	1.62 ± 0.26	1.66 ± 0.25	0.038
Relation to pleura	1.Attachment	Negative retraction (–)	6 17	20 48	26 65	< 0.001
	2.Tags		11	28	39	
	3.Indentation	Positive retraction (+)	30	20	50	
Pleura thickening, *n* (%)			13 (27.7%)	10 (14.7%)	23 (20%)	0.740

Data are numbers (%) and mean ± standard deviation

RUL right upper lobe, *RML* right middle lobe, *RLL* right lower lobe, *LUL* left upper lobe, *LLL* left lower lobe

were restricted to solid or part-solid lesions, with none concerning pGGNs. Si et al [42] concluded that the presence of pleural retraction may preclude atypical adenomatous hyperplasia (AAH) from AIS and MIA. Ahn et al [43] proposed that pleural contact, pleural thickening, solid proportion greater than 50% and nodule size greater than 20 mm were significant indicators of VPI by T1-sized peripheral mGGN-like adenocarcinomas. In the present study, we investigated the existence and diagnosis of VPI in malignant pGGNs for the first time with a result indicating that this indolent tumour generally does not invade the pleura, regardless of tumour size, morphology, (relative) density or tumour–pleura interaction. This conclusion can to a great extent dismiss the worries about VPI in pGGNs preoperatively and facilitate clinical decision-making.

We also assessed the significance of pleural morphological change to predict IA by classifying the lesions into three representative categories [30–33]. In the univariate analysis, the rate of pleural indentation was significantly higher in the IA group than the pre-IA/MIA group ($p < 0.001$), while the other two types of tumour–pleural relationship were not differently distributed. We then defined pleural indentation as positive retraction, and the other two combined as negative retraction. Under this definition, pleural retraction was the most significant independent risk factor of IA in the subsequent multivariate analysis (OR = 5.663, $p < 0.001$).

On the other hand, higher tumour density and greater proportion of solid component were also reported as independent predictors for IA in mGGNs [10, 44, 45]. In the present study, we also take fully into account the

Table 3 Independent predictors of pleural invasion in the multivariate logistic regression analysis (backward conditioning) and the ORs of the retained variables

Variate	Significance	OR	95% confidence interval of OR
Pleural retraction	< 0.001	5.66	[2.26, 14.20]
Lobulated shape	0.016	4.81	[1.34, 17.33]
Relative density (> 1.60)	0.001	4.45	[1.79, 11.06]

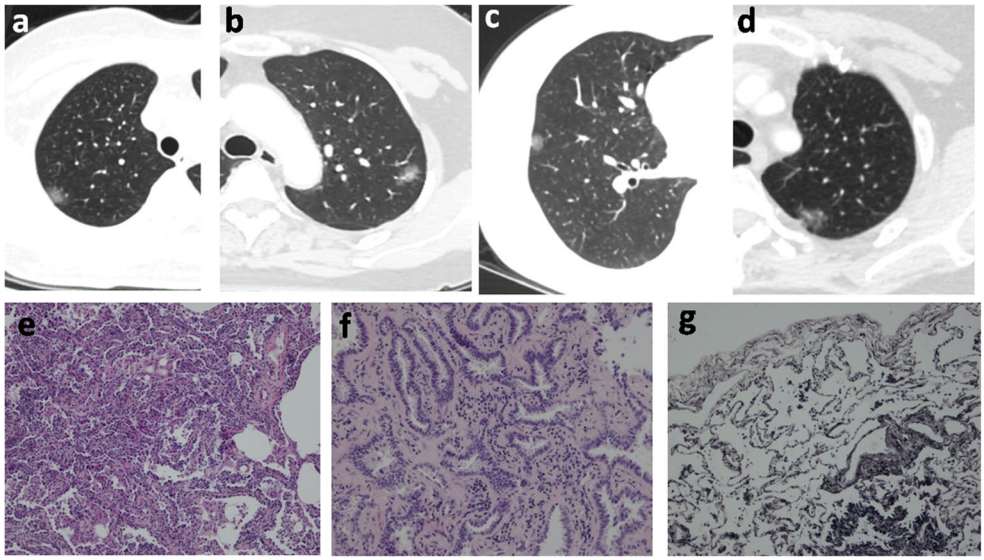

Fig. 2 Relationship of CT manifestation and pGGN invasiveness. **a** Slightly lobulated pGGN in the RUL, with pleural attachment and a relative density of 1.54, tuned out to be an MIA. **b** Lobulated pGGN in the LUL, showing multiple pleural tags radiating to the pleura costalis without causing pleural folding, with a relative density of 1.69, proved to be an IA. **c** Round pGGN in the RML, with pleural attachment and a relative density of 1.46, was confirmed as an AIS in the subsequent pathological examination (**d**, HE, ×200). **e** Lobulated pGGN in the LUL, causing tentiform retraction of the pleura into the tumour, with a relative density of 1.67. The pathologic examination proved it an acinar-predominant IA (**f**, HE, ×200), and the Elastica–Masson staining (**g**, ×200) showed the pleura was intact without tumour infiltration (PL0)

influence of tumour density. Because of the study's retrospective nature, some of the enrolled patients received a contrast-enhanced CT scan while others underwent a non-enhanced procedure. To eliminate the confounding of contrast agent and reduce the impact of respiratory status, we introduced a new concept of "relative density" as described in our previous study [27], calculated by comparing the CT attenuation of the lesion to the normal lung tissue. In the univariate analysis, a significantly higher relative density was observed in the IA group than pre-IA/MIA group (1.72 ± 0.24 vs. 1.62 ± 0.26, p = 0.038). The subsequent ROC analysis and multivariate regression study further demonstrated that a relative density greater than 1.60 can increase the risk of IA in pGGNs by 4.4 times (p = 0.001).

Lobulated shape, coarse interface [11, 46–48] and large tumour size [6, 8, 44–47] are well-known, important CT characteristics to distinguish IA. Pathologically, malignant lobulation is caused by different growth force owing to different cell differentiation, tumour growth blocked by the adjacent pulmonary interstitium and contraction of fibrous tissue inside the lesion [49]. In the present study, the incidence of lobulation was significantly higher in the IA group (91.5% vs. 69.1%, p = 0.004), and it was also proved to be an independent predictor of IA with an increased risk by 4.8 times (p = 0.016). Nevertheless, in this study, although IA preferred a coarse contour and larger diameter, the differences were not statistical significant (p = 0.253 and 0.679, respectively). These insignificancies may be attributed to the essence of a single-centre study and tumour location, as the lung cancer screening project in our hospital increased the detection of small and early lesions, thus resulting in bias of the tumour size; whereas subpleural location may conceal part of the tumour interface.

The present study still has several limitations. Firstly, this study was of retrospective design, so there may be observation and examination bias. For example, the cases enrolled were only pathologically proven malignant pGGNs, without considering the differentiation with benign lesions, and the CT examinations were not able to achieve consistency with regard to the use of contrast agent. While the objective of our study was to distinguish the invasiveness of malignant pGGNs, so the question about "benign or malignant" should be answered, maybe by surveillance or other methods, before applying our conclusions. On the other hand, the introduction of relative density can greatly reduce the confounding of contrast agent. Secondly, this was a single-centre study, and the diagnostic performance was not high enough. So, further studies incorporating multicentre cases or of prospective design are desirable. In addition, it is expected that artificial intelligence and radiomic methodology can be applied to improve the predictive capability.

In summary, the present study showed that pulmonary adenocarcinoma manifesting as pGGN generally does not invade the pleura. A comprehensive consideration of tumour shape, relative density and tumour–pleural relationship can independently predict IA.

Funding This study has received funding by the National Natural Science Foundation of China (Grant No. 81171344).

Compliance with ethical standards

Guarantor The scientific guarantor of this publication is Jian-wei Wang.

Conflict of interest The authors of this manuscript declare no relationships with any companies whose products or services may be related to the subject matter of the article.

Statistics and biometry No complex statistical methods were necessary for this paper.

Informed consent Written informed consent was waived by the institutional review board.

Ethical approval Institutional review board approval was obtained.

Methodology
- retrospective
- diagnostic, observational
- performed at one institution

References

1. Bak SH, Lee HY, Kim JH et al (2016) Quantitative CT scanning analysis of pure ground-glass opacity nodules predicts further CT scanning change. Chest 149:180–191
2. Yip R, Henschke CI, Xu DM et al (2017) Lung cancers manifesting as part-solid nodules in the national lung screening trial. AJR Am J Roentgenol 208:1011–1021
3. Austin JH, Muller NL, Friedman PJ et al (1996) Glossary of terms for CT of the lungs: recommendations of the Nomenclature Committee of the Fleischner Society. Radiology 200:327–331
4. Kim HY, Shim YM, Lee KS et al (2007) Persistent pulmonary nodular ground-glass opacity at thin-section CT: histopathologic comparisons. Radiology 245:267–275
5. Travis WD, Brambilla E, Nicholson AG et al (2015) The 2015 World Health Organization classification of lung tumors: impact of genetic, clinical and radiologic advances since the 2004 classification. J Thorac Oncol 10:1243–1260
6. Lim HJ, Ahn S, Lee KS et al (2013) Persistent pure ground-glass opacity lung nodules >/= 10 mm in diameter at CT scan: histopathologic comparisons and prognostic implications. Chest 144: 1291–1299
7. Ichinose J, Kohno T, Fujimori S et al (2014) Invasiveness and malignant potential of pulmonary lesions presenting as pure ground-glass opacities. Ann Thorac Cardiovasc Surg 20:347–352
8. Moon Y, Sung SW, Lee KY, Sim SB, Park JK (2016) Pure ground-glass opacity on chest computed tomography: predictive factors for invasive adenocarcinoma. J Thorac Dis 8:1561–1570
9. Lee HY, Choi YL, Lee KS et al (2014) Pure ground-glass opacity neoplastic lung nodules: histopathology, imaging, and management. AJR Am J Roentgenol 202:W224–W233
10. Zhang Y, Shen Y, Qiang JW et al (2016) HRCT features distinguishing pre-invasive from invasive pulmonary adenocarcinomas appearing as ground-glass nodules. Eur Radiol 26:2921–2928
11. Wu F, Tian SP, Jin X et al (2017) CT and histopathologic characteristics of lung adenocarcinoma with pure ground-glass nodules 10 mm or less in diameter. Eur Radiol 27:4037–4043
12. Nemec U, Heidinger BH, Anderson KR et al (2018) Software-based risk stratification of pulmonary adenocarcinomas manifesting as pure ground glass nodules on computed tomography. Eur Radiol 28:235–242
13. Son JY, Lee HY, Kim JH et al (2016) Quantitative CT analysis of pulmonary ground-glass opacity nodules for distinguishing invasive adenocarcinoma from non-invasive or minimally invasive adenocarcinoma: the added value of using iodine mapping. Eur Radiol 26:43–54
14. Jiang L, Liang W, Shen J et al (2015) The impact of visceral pleural invasion in node-negative non-small cell lung cancer: a systematic review and meta-analysis. Chest 148:903–911
15. Shimizu K, Yoshida J, Nagai K et al (2005) Visceral pleural invasion is an invasive and aggressive indicator of non-small cell lung cancer. J Thorac Cardiovasc Surg 130:160–165
16. Kudo Y, Saji H, Shimada Y et al (2012) Impact of visceral pleural invasion on the survival of patients with non-small cell lung cancer. Lung Cancer 78:153–160
17. Nitadori J, Colovos C, Kadota K et al (2013) Visceral pleural invasion does not affect recurrence or overall survival among patients with lung adenocarcinoma </= 2 cm: a proposal to reclassify T1 lung adenocarcinoma. Chest 144:1622–1631
18. Yanagawa N, Shiono S, Abiko M et al (2013) Prognostic impact and initial recurrence site of lymphovascular and visceral pleural invasion in surgically resected stage I non-small-cell lung carcinoma. Eur J Cardiothorac Surg 44:e200–e206
19. Neri S, Yoshida J, Ishii G et al (2014) Prognostic impact of microscopic vessel invasion and visceral pleural invasion in non-small cell lung cancer: a retrospective analysis of 2657 patients. Ann Surg 260:383–388
20. Adachi H, Tsuboi M, Nishii T et al (2015) Influence of visceral pleural invasion on survival in completely resected non-small-cell lung cancer. Eur J Cardiothorac Surg 48:691–697 discussion 697
21. Huang H, Wang T, Hu B, Pan C (2015) Visceral pleural invasion remains a size-independent prognostic factor in stage I non-small cell lung cancer. Ann Thorac Surg 99:1130–1139
22. Liu QX, Deng XF, Zhou D et al (2016) Visceral pleural invasion impacts the prognosis of non-small cell lung cancer: a meta-analysis. Eur J Surg Oncol 42:1707–1713
23. Oyama M, Miyagi Maeshima A, Tochigi N et al (2013) Prognostic impact of pleural invasion in 1488 patients with surgically resected non-small cell lung carcinoma. Jpn J Clin Oncol 43:540–546
24. Suzuki K, Koike T, Asakawa T et al (2011) A prospective radiological study of thin-section computed tomography to predict pathological noninvasiveness in peripheral clinical IA lung cancer (Japan Clinical Oncology Group 0201). J Thorac Oncol 6:751–756
25. Hattori A, Suzuki K, Matsunaga T, Takamochi K, Oh S (2014) Visceral pleural invasion is not a significant prognostic factor in patients with a part-solid lung cancer. Ann Thorac Surg 98:433–438
26. Hansell DM, Bankier AA, MacMahon H et al (2008) Fleischner Society: glossary of terms for thoracic imaging. Radiology 246: 697–722
27. Qi LL, Wang JW, Yang L et al (2017) The role of volume and mass doubling times of pulmonary pure ground glass nodules in differentiating invasive adenocarcinomas from minimally invasive adenocarcinomas and preinvasive lesions. Chin J Radiol 51:7
28. Chen B, Barnhart H, Richard S et al (2013) Volumetric quantification of lung nodules in CT with iterative reconstruction (ASiR and MBIR). Med Phys 40:111902
29. Kim H, Park CM, Woo S et al (2013) Pure and part-solid pulmonary ground-glass nodules: measurement variability of volume and mass in nodules with a solid portion less than or equal to 5 mm. Radiology 269:585–593

30. Liu Y, Kim J, Qu F et al (2016) CT features associated with epidermal growth factor receptor mutation status in patients with lung adenocarcinoma. Radiology 280:271–280
31. Qi LP, Li XT, Yang Y et al (2016) Multivariate analysis of pleural invasion of peripheral non-small cell lung cancer-based computed tomography features. J Comput Assist Tomogr 40:757–762
32. Hsu JS, Han IT, Tsai TH et al (2016) Pleural tags on CT scans to predict visceral pleural invasion of non-small cell lung cancer that does not abut the pleura. Radiology 279:590–596
33. Cohen JG, Reymond E, Lederlin M et al (2015) Differentiating pre- and minimally invasive from invasive adenocarcinoma using CT-features in persistent pulmonary part-solid nodules in Caucasian patients. Eur J Radiol 84:738–744
34. Travis WD, Brambilla E, Rami-Porta R et al (2008) Visceral pleural invasion: pathologic criteria and use of elastic stains: proposal for the 7th edition of the TNM classification for lung cancer. J Thorac Oncol 3:1384–1390
35. Fisseler-Eckhoff A (2009) New TNM classification of malignant lung tumors 2009 from a pathology perspective. Pathologe 30 (Suppl 2):193–199
36. Cicchetti DV, Sparrow SA (1981) Developing criteria for establishing interrater reliability of specific items: applications to assessment of adaptive behavior. Am J Ment Defic 86:127–137
37. Fujimoto T, Cassivi SD, Yang P et al (2006) Completely resected N1 non-small cell lung cancer: factors affecting recurrence and long-term survival. J Thorac Cardiovasc Surg 132:499–506
38. Suzuki K, Nagai K, Yoshida J, Nishimura M, Nishiwaki Y (2001) Predictors of lymph node and intrapulmonary metastasis in clinical stage IA non-small cell lung carcinoma. Ann Thorac Surg 72:352–356
39. Ebara K, Takashima S, Jiang B et al (2015) Pleural invasion by peripheral lung cancer: prediction with three-dimensional CT. Acad Radiol 22:310–319
40. Imai K, Minamiya Y, Ishiyama K et al (2013) Use of CT to evaluate pleural invasion in non-small cell lung cancer: measurement of the ratio of the interface between tumor and neighboring structures to maximum tumor diameter. Radiology 267:619–626
41. Meniga IN, Tiljak MK, Ivankovic D et al (2010) Prognostic value of computed tomography morphologic characteristics in stage I non-small-cell lung cancer. Clin Lung Cancer 11:98–104
42. Si MJ, Tao XF, Du GY et al (2016) Thin-section computed tomography-histopathologic comparisons of pulmonary focal interstitial fibrosis, atypical adenomatous hyperplasia, adenocarcinoma in situ, and minimally invasive adenocarcinoma with pure ground-glass opacity. Eur J Radiol 85:1708–1715
43. Ahn SY, Park CM, Jeon YK et al (2017) Predictive CT features of visceral pleural invasion by T1-sized peripheral pulmonary adenocarcinomas manifesting as subsolid nodules. AJR Am J Roentgenol 209:561–566
44. Lee SM, Park CM, Goo JM et al (2013) Invasive pulmonary adenocarcinomas versus preinvasive lesions appearing as ground-glass nodules: differentiation by using CT features. Radiology 268:265–273
45. Lee SM, Goo JM, Lee KH et al (2015) CT findings of minimally invasive adenocarcinoma (MIA) of the lung and comparison of solid portion measurement methods at CT in 52 patients. Eur Radiol 25:2318–2325
46. Godoy MC, Naidich DP (2009) Subsolid pulmonary nodules and the spectrum of peripheral adenocarcinomas of the lung: recommended interim guidelines for assessment and management. Radiology 253:606–622
47. Lee HJ, Goo JM, Lee CH et al (2009) Predictive CT findings of malignancy in ground-glass nodules on thin-section chest CT: the effects on radiologist performance. Eur Radiol 19:552–560
48. Fan L, Liu SY, Li QC, Yu H, Xiao XS (2012) Multidetector CT features of pulmonary focal ground-glass opacity: differences between benign and malignant. Br J Radiol 85:897–904
49. Winer-Muram HT (2006) The solitary pulmonary nodule. Radiology 239:34–49